

SymFace: Additional Facial Symmetry Loss for Deep Face Recognition

Pritesh Prakash
 Central Research Laboratory
 Bharat Electronics Limited
 Ghaziabad, India, 201010
 priteshpakash@bel.co.in

Koteswar Rao Jerripothula
 Department of Electrical Engineering
 IIT Kanpur
 India, 208016
 kotesrj@iitk.ac.in

Ashish Jacob Sam
 Central Research Laboratory
 Bharat Electronics Limited
 Ghaziabad, India, 201010
 ashishjacobsam@bel.co.in

Prinsh Kumar Singh
 Central Research Laboratory
 Bharat Electronics Limited
 Ghaziabad, India, 201010
 prinshkumarsingh@bel.co.in

S Umamaheswaran
 Central Research Laboratory
 Bharat Electronics Limited
 Ghaziabad, India, 201010
 sumamaheswaran@bel.co.in

Abstract

Over the past decade, there has been a steady advancement in enhancing face recognition algorithms leveraging advanced machine learning methods. The role of the loss function is pivotal in addressing face verification problems and playing a game-changing role. These loss functions have mainly explored variations among intra-class or inter-class separation. This research examines the natural phenomenon of facial symmetry in the face verification problem. The symmetry between the left and right hemifaces has been widely used in many research areas in recent decades. This paper adopts this simple approach judiciously by splitting the face image vertically into two halves. With the assumption that the natural phenomena of facial symmetry can enhance face verification methodology, we hypothesize that the two output embedding vectors of split faces must project close to each other in the output embedding space. Inspired by this concept, we penalize the network based on the disparity of embedding of the symmetrical pair of split faces. Symmetrical loss has the potential to minimize minor asymmetric features due to facial expression and lighting conditions, hence significantly increasing the inter-class variance among the classes and leading to more reliable face embedding. This loss function propels any network to outperform its baseline performance across all existing network architectures and configurations, enabling us to achieve SoTA results.

1. Introduction

The symmetry between the left and right hemifaces is a natural phenomenon. Absolute symmetry between the two sides of faces can be rare, but it's also uncommon to find someone with a highly asymmetrical face. The degree of symmetry varies from person to person; some may possess a highly symmetrical face, while others may not. Facial asymmetry can stem from various factors, including genetic predispositions, developmental irregularities, traumatic incidents, or other influences impacting the formation and growth of facial structures. These factors can result in visible differences in the positioning and proportions of facial features such as the eyes, nose, mouth, and ears, which are often noticeable in cases of facial asymmetry. The study of face symmetry holds a significant backbone in many research domains. Researchers usually utilize facial symmetry as a metric for assessing attractiveness [1, 2], gauging emotional expressions [3], investigating neurological disorders [4] and Deepfake analysis [5]; its applications span across fields like psychology, anthropology, and medicine, offering insights into various aspects of human biology, behavior, and perception etc.

Due to the association of symmetrical behaviour between the left and right hemifaces, we applied the symmetrical influence in the existing face recognition methods. Measuring symmetry in face data is only feasible if the camera is positioned appropriately in front of the face. Although projecting from 3D to 2D loses some symmetrical aspects, there is still enough symmetrical information retained in the 2D images from the analysis. The available face datasets [6, 7] consist of face images captured from various angles and positions (Fig. 1), causing a significant variance in the



(a) Samples with good symmetrical features (b) Samples with poor symmetrical features

Figure 1. Symmetrical analysis on face dataset

view angle and orientation of the face. This is a natural occurrence but imposes a real hindrance in existing face recognition datasets and may affect the ability of the network to learn the symmetrical factors in the face recognition problem. If we analyze the faces at extreme view angles, it is observed that the mind barely recognizes the symmetry between the hemi faces. In such cases, only one hemi face is visible. Therefore, we do not derive the symmetrical factors from such images, which are tilted more than a marginal angle. However, we feed these images to the network without adding the symmetrical aspects. This approach allows us to apply the symmetrical effect only to well-oriented face images. This way, the network learns to extract the asymmetric features more precisely from the image and outperforms the benchmarks in side pose datasets [8, 9].

We’ve developed a standard technique called the 3-Point Symmetric Split (3PSS) algorithm for assessing and assigning symmetric orientation coefficient (ρ) in facial features. A high value of ρ implies a good orientation for detecting symmetry, and a lower value of ρ implies a poor orientation for detecting symmetry in facial features. The 3PSS algorithm is designed to analyze symmetrical orientation in 2D space. Consequently, images may get classified as lower ρ because of the face orientation in the 2D space, despite the individual having a naturally symmetrical face. While 3PSS provides valuable insights into facial symmetry, its application can be limited to specific types of research, and it is advised to avoid erroneous conclusions. The 3PSS algorithm categorizes each image of datasets as symmetrical or asymmetrical with a corresponding ρ value.

In the past decade, various novel approaches have been explored to enhance the discriminating power of the network and demonstrate outstanding results in the face recognition domain. The main principle behind the previous research is to increase inter-class and reduce the intra-class variation among the classes. The network output, i.e., the positioning of the vector embedding in the embedding space of two input images of the same class, should be projected close to each other. So, we hypothesize that the vertically split faces of the same person belonging to the same input will also be projected much closer to each other in the em-

bedding space. With this hypothesis, we introduce an innovative method for integrating SymFace loss. The network can be trained to minimize the distance between any complete facial feature and hemi faces belonging to the same class. Adding the SymFace loss with the standard face losses achieves SoTA results in various networks and surpasses the existing benchmark datasets [8–12] in the face recognition domain.

The key feature of the proposed method can be summarized as:

- We introduce the influence of facial symmetry in the face recognition domain. In this proposed methodology, we define a systematic approach to apply SymFace loss from the data augmentation to the loss calculation.
- We propose a method that navigates the 2-D space, significantly reducing manual effort and computational overhead in exploring symmetry. However, this method is not recommended for measuring symmetry in the face for any generic purposes.
- We propose a theory that the vertically split front 2-D face image possesses the property of symmetry, and two symmetrical halves should be close enough to each other in the output embedding space, implying that the L2 distance between the embedding of the two halves of such hemi faces should be minimal.
- We add the SymFace loss to any generic face loss. The aggregated loss tends to aid the network in extracting the hidden information of asymmetry and helps to increase the inter-class variance among the classes.
- We evaluate the added SymFace loss with various datasets (LFW, CFP-FP, CP-LFW, AgeDB, CA-LFW), and their results indicate the excellent potential of SymFace loss in the face recognition tasks.

2. Literature Review

The symmetrical behavior in face recognition solutions has been explored in the past. The paper [13] explores how facial asymmetry affects facial recognition, focusing on expression variations, gender classification, and expression differentiation. The input images were computed using density difference (D-face) and edge orientation symmetry (S-face) to measure the asymmetry score. The author used principal component analysis to reduce the dimensions and performed the classification using the linear discriminant analysis (LDA) method. The other approach [14] proposed a technique to enhance face recognition accuracy under occlusions and varying lighting. It integrates Local Binary

Patterns (LBP) with multi-mirror symmetry to capture facial textures and leverage reflective properties. The process includes pre-processing images, calculating LBP histograms, and combining them with mirrored facial features for recognition using a nearest-neighbor classifier. The paper [15] calculated the difference between the right and left half-face images in the input space and tried to classify facial images using the calculated difference along with other attributes of the person.

Advanced neural network methods in face recognition have been brought from diverse spheres of the domain. One area of particular importance is enhancing loss functions in face recognition. The classification task involves the evaluation of Softmax loss obtained from the images and their corresponding labels, as shown:

$$\mathcal{L}_{\text{CE}}(x_i) = -\log \frac{\exp(W_{y_i} z_i)}{\sum_{j=1}^C \exp(W_j z_i)} \quad (1)$$

Here, the i -th image sample x_i is assigned label y_i out of total classes C , and the embedding of x_i is $z_i \in R^d$, where d is the embedding size. The weight matrix is $W \in R^{d \times C}$, and the bias terms are set to zero.

Advancing from Softmax [16–18], then employing weight and embedding normalization [19–21], led the research community into angular space

$$\mathcal{L}_{\text{CE}}(x_i) = -\log \frac{\exp(s(\cos \theta_{y_i}))}{\sum_{j=1}^C \exp(s(\cos \theta_j))} \quad (2)$$

Here, θ is the angle between the feature z_i and the weight W_j , and s is the scaling factor in the angular space.

This forged a new frontier in face recognition. With this new approach, the margin played a crucial role in cosine space (Eq. 3) [22], multiplication (Eq. 4) [23] and addition (Eq. 5) [24] of the margin in theta space instead of cosine space exhibiting outstanding results.

$$L_{\text{CosFace}} = -\log \frac{\exp(s \cos(\theta_{y_i}) - m)}{\exp(s(\cos(\theta_{y_i}) - m)) + \sum_{j=1, j \neq y_i}^N \exp(s \cos \theta_j)} \quad (3)$$

$$L_{\text{SphereFace}} = -\log \frac{\exp(s \cos(\theta_{y_i} \times m))}{\exp(s \cos(\theta_{y_i} \times m)) + \sum_{j=1, j \neq y_i}^N \exp(s \cos \theta_j)} \quad (4)$$

$$L_{\text{ArcFace}} = -\log \frac{\exp(s \cos(\theta_{y_i} + m))}{\exp(s \cos(\theta_{y_i} + m)) + \sum_{j=1, j \neq y_i}^N \exp(s \cos \theta_j)} \quad (5)$$

In (Eq. 3 - Eq. 5), θ_{y_i} the most pivotal variable m is the margin for adding the penalty.

The strategy used by [25] was training with lower margins for easy samples and higher margins for complex samples, emphasizing the practical nature of adaptiveness during the training cycles. AdaFace [26] further emphasized the easy and hard samples based on image quality and utilized feature normalization for the quality assessment. We are simply introducing a loss function that can be added easily to any existing loss functions and help the combined face loss function be more powerful. Our proposed symmetrical loss function extends this approach by incorporating a natural phenomenon of facial symmetry into the cosine space. While traditional losses enhance embedding through angular margins, they do not explicitly leverage the inherent symmetry present in human faces. By integrating symmetry constraints into the cosine similarity framework, our method refines the embedding in a manner that aligns more closely with natural facial structures.

Better results require a better network, and many network architectures are proposed to improve face recognition results. In the current scenario, mobile-based networks have become essential due to their widespread applications in autonomous vehicles, robotics, and unmanned aerial vehicles (UAVs). Tailoring the networks for edge devices necessitates considering their lower computational requirements [27–33], specifically regarding floating-point operations (FLOPs), and a reduction in parameters. While many networks have been proposed to address these requirements in face verification, [34–37], achieving the anticipated results remains challenging. Some networks [35, 38] have managed to reduce FLOPs, thereby improving computational efficiency, but at the expense of higher numbers of parameters. Conversely, networks [32] with lower parameter counts often entail higher FLOPs, which is a trade-off dilemma. This underscores the need for innovative approaches to balance computational efficiency and model complexity. This research incorporates the proposed SymFace loss into existing lightweight face recognition architectures and presents significant advancements in their performance.

The ResNet50 and ResNet100 architectures have performed remarkably in various newly developed face recognition methods [39–43]. But ResNet100 trained on MS1M-V2 has staggered with 99.82% accuracy in LFW. Enhancing the loss function can elevate any network’s capacity to discern and distinguish facial features more precisely. Other methods such as BroadFace [44] optimizes face recognition by leveraging a linear classifier to consider a vast array of identities. The advancement in probabilistic face embeddings [45] by Sphere Confidence Face [46] computes the confidence learning in spherical space from the Euclidian space. Such refinement could potentially lead to significant improvements in accuracy and performance, ultimately advancing the capabilities of face recognition systems for var-

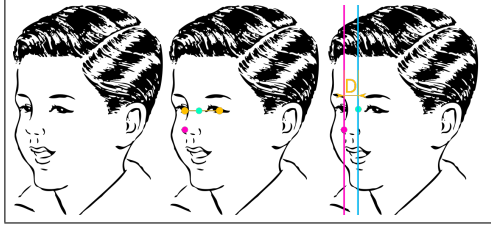


Figure 2. Images being evaluated by the 3PSS

Source: Pixabay, Free for use under the Pixabay Content License

ious applications, including security, surveillance, biometrics, etc.

3. Proposed Method

To leverage facial symmetry in developing a face recognition model, we introduce a facial frontness measure, denoted as ρ , to identify images that capture a frontal view of the face. We then split these images into two parts to generate separate embeddings, which are expected to be similar. This similarity is enforced using our additional facial symmetry loss, SymFace. This section describes our novel 3PSS (3-point symmetric split) algorithm, which measures facial frontness and performs image splitting. We will then explain how the SymFace loss is utilized during model training.

3.1. 3PSS

3.1.1 Facial Frontness Measurement

We extract three facial landmarks, namely two eyes and a nose, using a pre-trained RetinaFace [47] model. We denote the x-coordinate of the landmarks of the left and right eyes as e_x^l and e_x^r , respectively, and of the nose as n_x . The x-coordinate of the midpoint of the two eyes should be close to that of the nose to consider that the image has a frontal view of the face. A significant discrepancy in the two values suggests that either the face is tilted or not frontal, making it impractical to split the face. Thus, we calculate this discrepancy (denoted as D) as follows:

$$D = \left| n_x - \frac{(e_x^l + e_x^r)}{2} \right|, \quad (6)$$

which we use to compute what we call symmetric orientation coefficient(ρ) in the following manner:

$$\rho = \frac{1}{1 + D^2} \quad (7)$$

These steps can be visualized in Figure 6, shown on a face-sketch along with landmarks of eyes (denoted in yellow dots) and nose(magenta dot).



(a) Sample with score 0.01 (b) Sample with score 0.38 (c) Sample with score 0.5

Figure 3. A comparison of ρ various images from the dataset

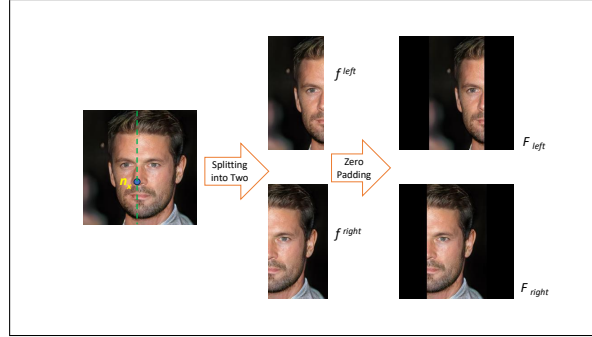


Figure 4. Face Image Splitting Process

Note that we designate the ρ value as zero for images where the landmark detector (RetinaFace) fails to detect landmarks.

3.1.2 Image Splitting

From Eq. (7), it's clear that the lower the discrepancy D , the higher the ρ value. Thus, images with higher values of ρ will be preferred for selecting frontal face images.

We use a threshold ρ with τ (set as 0.2) to determine whether an image qualifies as symmetric or not, i.e., images with $\rho > \tau$ are considered "symmetric"; otherwise, and "asymmetric" otherwise. However, splitting every qualified image is undesirable because the network would never be trained on a full symmetric face image in such a case, and it would also increase the number of images more than required. So, only a fraction p (set as 0.3) of these images are split in any epoch.

Images in Fig. 3 show faces with various values of ρ . Fig. 3a is considered asymmetrical due to its low ρ value, whereas Fig. 3b and Fig. 3c are considered symmetrical.

For all images categorized as symmetric, we vertically split the face images into two halves: f^{left} and f^{right} for all images using n_x , the x-coordinate of nose landmark. While f^{left} denotes the part of the image with columns up to n_x , f^{right} denotes the remaining part. Both these parts are converted into an image of the same size as that of the original image by zero padding, such that they are at the center of the resulting images, F_{left} and F_{right} , as shown in the Fig. 4.

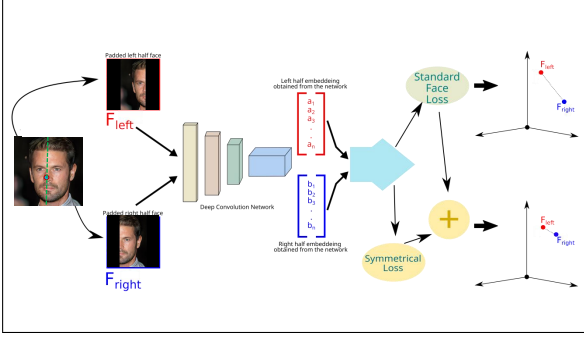


Figure 5. Workflow of split samples

3.2. Training Procedure

3.2.1 Training Samples

In any epoch, with a fraction of randomly selected symmetrical images split, the number of training samples (N) in any epoch is increased as shown:

$$\begin{aligned}
 N' &= N_{asym} + (1 - p)N_{sym} + 2pN_{sym} \\
 &= N_{asym} + (1 + p)N_{sym} \\
 &= N + pN_{sym}
 \end{aligned} \tag{8}$$

where N_{sym} can be defined as follows:

$$N_{sym} = \sum_{i=1}^N \delta(\rho_i > \tau), \tag{9}$$

where i is the index of the image in the original dataset. In any epoch, there will be two types of samples: full and half images. The full images are denoted as x_i , and the half images are denoted as x_i^l or x_i^r for left and right face images. Let $h_i \in \{0, 1\}$ denote whether the full image x_i has been split into x_i^l and x_i^r or not in a given epoch.

3.2.2 SymFace Loss

Our SymFace loss is defined as follows:

$$\mathcal{L}_\rho = \frac{1}{2pN_{sym}} \sum_{i=1}^N \rho_i \delta(h_i) \|E(x_i^l) - E(x_i^r)\|_2^2 \tag{10}$$

Here, $E(x)$ denotes the output embedding of the face recognition network for image x . The idea is to apply our new loss only to the selected images out of the qualified ones for splitting. As shown in Fig. 5, this loss tries to bring the two embeddings closer.

3.2.3 Generic Face Loss

Let the standard loss function be denoted as $L_f(x, y)$ for a single sample, where x is the image and y is the image label. Our generic face loss can now be defined as follows:

$$\mathcal{L}_f = \frac{1}{N'} \sum_{i=1}^N \delta(!h_i) L_f(x_i, y_i) + \delta(h_i) (L_f(x_i^l, y_i) + L_f(x_i^r, y_i)) \tag{11}$$

Note that the denominator is N' , not N because the loss is optimized for both full and half images.

3.2.4 Total Loss

Finally, we combine the two losses discussed to arrive at our final loss:

$$\mathcal{L}_{total} = \mathcal{L}_f + \mathcal{L}_\rho \tag{12}$$

4. Experiments

4.1. Datasets

We use the MS1MV2 dataset for the training cycle containing 5.8M facial images of 85K identities, and Web-face [48] containing 4.2M facial images. The images in the dataset are first tagged with three facial landmarks using a pre-trained RetinaFace model [47]. These three landmark points, which include two eyes and one nose point, along with ρ value against each image, are used as input along with the image data.

The validation cycle includes the following datasets: the LFW dataset [10] containing 13,233 facial images of 5,749 people, the CFP-FP [8] dataset containing 7,000 facial images of 500 people, the CP-LFW [9] dataset contains 11,652 images of 5,749 people, the AgeDB [11] dataset contains 16,488 facial images of 568 people, and the CA-LFW [12] dataset contains 12,174 facial images of 5,749 people.

4.2. Experimental Settings

In this experiment, the SymFace loss is used as an additional loss on top of existing loss functions ArcFace [24] and AdaFace [26]. The final combined loss is used during the training phase. We use different networks in this experiment to test the impact of SymFace loss. We use two lightweight networks, MobileFaceNet [34] with 0.99M parameters and ShuffleFaceNet [36] with 2.6M parameters, as network backbones. We also use Resnet50 and ResNet100, as discussed in [24], as heavy network backbone.

We use 3 A100 NVIDIA GPUs for lightweight networks and 8 A100 GPUs for heavy networks. As we make pairs in the dataset class, the batch size for lightweight networks is 75, while for heavy networks, it is 256. The network is fed with concatenated tensors, increasing the total batch

Configuration			Validation Dataset	
Model	Loss	Train Data	LFW	AgeDB
MobileFaceNet [34]	ArcFace	CASIA-WebFace 112X96	99.18	92.96
	ArcFace+SymFace		99.31	91.06
MobileFaceNet [34]	ArcFace	MS1MV2	99.55	96.07
	ArcFace+SymFace		99.65	96.08
ShuffleFaceNet x1.5 [36]	ArcFace	MS1MV2	99.67	97.32
	ArcFace+SymFace		99.73	96.71

Table 1. Verification performance (%) on Lightweight Networks with the embedding size of 128

Configuration			Validation Dataset				
Model	Train Data	Loss	LFW	AgeDB	CA-LFW	CP-LFW	CFP-FP
ResNet50	MS1MV2	AdaFace [26]	99.82	97.85	96.07	92.83	97.86
		AdaFace+SymFace	99.83	97.89	96.09	93.29	98.30
ResNet100	MS1MV2	AdaFace [26]	99.82	98.05	96.08	93.53	98.49
		AdaFace+SymFace	99.85	98.08	96.14	93.14	98.30
ResNet100	MS1MV2	CosFace [26]	99.81	98.11	95.76	92.28	98.12
		CosFace+SymFace	99.83	98.04	96.08	93.58	98.40
ResNet100	MS1MV2	ArcFace	99.83	98.28	95.45	92.08	98.27
		ArcFace+SymFace	99.82	98.01	95.99	93.06	98.25
ResNet50	WebFace4M	AdaFace [26]	99.78	97.78	95.98	94.17	98.97
		AdaFace+SymFace	99.83	97.86	96.01	94.66	99.01
ResNet100	WebFace4M	CosFace [48]	99.80	97.45	95.95	94.40	99.25
		CosFace+SymFace	99.83	97.81	95.84	94.46	99.15
ResNet100	WebFace4M	ArcFace [49]	99.83	98.28	95.45	92.08	98.27
		ArcFace+SymFace	99.83	97.61	96.01	94.21	99.06
ResNet100	WebFace4M	AdaFace [26]	99.80	97.90	96.05	94.63	99.17
		AdaFace+SymFace	99.85	97.83	95.93	94.53	99.20

Table 2. Verification performance (%) on ResNet 50 and ResNet 100 with the embedding size 512

sizes to 150 and 512 for lightweight and heavy networks, respectively. For lightweight networks and ResNet50, the network is trained up to 25 epochs. For ResNet100, the total number of epochs is set as 12. The initial learning rate is set as 0.1 for lightweight networks, and step scheduling is set at 17 (0.01). The initial learning rate for ResNet50 and ResNet100 is set at 0.01 and step scheduling at 10 (0.001). The SGD optimizer (momentum = 0.9) is used with weight decay as $4e-5$ and $5e-4$ for lightweight and heavy networks, respectively. Only for the last layer of MobileFaceNet the weight decay is set as $4e-4$, as discussed in the paper [34].

AdaFace and ArcFace loss functions are combined with SymFace loss as shown in (Eq. 12). 128 and 512-sized embedding are used for lightweight and heavy networks, respectively. We normalize the image pixels by subtracting 127.5 and then dividing by 128. The horizontal flip is used during the training phase. For the lightweight networks with ArcFace+SymFace (ArcFace combined with SymFace) loss, the scale is set to 32, and the margin is 0.45. We do not add any augmentation (cropping, rescaling, and

photometric jittering) in this research as introduced by [26].

4.3. Comparison Results

For fair comparisons of the results, we perform the experiments to the baseline configurations (network and loss function) [24,26,34,36,50]. The SymFace loss improves the discriminating power of ArcFace and AdaFace and pushes the network for better convergence.

For MobileFaceNet and ShuffleFaceNet, we compute ArcFace+SymFace loss with an embedding size of 128. The results surpass 66 % of the times from the existing results as shown in Table 1. ResNet50 and ResNet100 are trained with additional SymFace loss and outperform the standard loss functions 70 % of the time, and their corresponding SoTA results are populated in Table 2. The proposed loss function outperforms the LFW dataset most of the time. ResNet50 backbone achieves better results than its counterpart in most validation datasets; on the other hand, the ResNet100 backbone achieves better results in LFW and age-related datasets when trained on MS1M V2 but gives

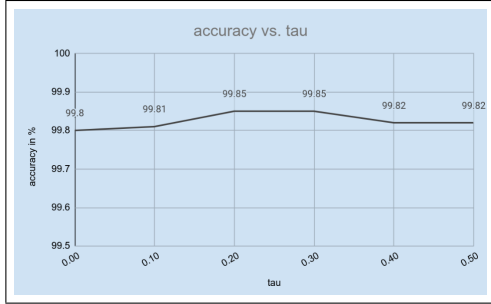


Figure 6. Accuracy Vs Tau

better results in side pose-related datasets when trained in the WebFace4M dataset.

4.4. Ablation Study

The network is trained with multiple values of τ , and it is observed that very low (less than 0.1) or very high (0.3 or higher) values of τ do not enhance model performance (refer Fig. 6). The network reports better results for ρ value in 0.2 ± 0.05 range. In our experiment, we find that feeding the network with the split augmentation but without symmetrical loss (only standard face loss) increases the model accuracy, but not up to the extent as with SymFace loss. When we train the ResNet100 network with split augmented images with standard loss only, it scores better at 99.82% compared to the base network’s accuracy of 99.8%. When the additional split images are fed to the ResNet100 network with additional symmetrical loss, we observe a better accuracy of 99.85% (refer Table 4). Combining standard face loss with symmetrical face loss outperforms most of the validation datasets. We also apply the SymFace loss to the CASIA-WebFace of size 112X96, and the accuracy on LFW increases from baseline results [51] of 99.18% to 99.31% (Table 1). To explore the potential of the natural phenomenon of symmetry, we train the VarGFaceNet from scratch on MS1MV2 without knowledge distillation, with AdaFace loss, and get an accuracy of 99.76 on the LFW dataset- compared to 99.67 % of the base model.

5. Discussion

The results on the WebFace4M dataset in Table 2 reveal that it outperforms pose variant datasets (CP-LFW and CFP-FP) compared to MS1M datasets. With the MS1MV2 dataset, the different loss functions scores in the range of 93.x % and 98.0x % in CP-LFW and CFP-FP datasets, respectively but WebFace4M scores in the higher range of 94.x % in CP-LFW and 99.x % in CFP-FP datasets. This behavior is because the WebFace dataset contains quality pose variant images for lower values of ρ (refer to Table 5). We analyze the improvement by the symmetrical loss for its discriminative capability of the network with better

feature representation of distinct face images. The inter-class variance for the CASIA-WebFace dataset is analyzed, and the symmetrical loss is noted to enhance the inter-class distances among the classes, as shown in Table 3. The explanation for this behavior is obvious: the network is generally assigned a penalty for finding asymmetry. Thus, the network learns to extract the hidden features of asymmetric information to generate the output embedding and can differentiate different classes based on these hidden asymmetrical features.

6. Conclusion

This paper discusses SymFace loss applied as an additional loss over standard face losses. To use this loss, the facial landmarks are identified using a pre-trained RetinaFace model, based on which we define our metric of face orientation, namely symmetric orientation coefficient, expressed as ρ . This allows us to group facial images based on 2D face properties to extract symmetric features. We also present a customized training process, in which we pass pairs of images (along with labels and their corresponding ρ values) and ensure that both types of facial images get processed by the total combined loss appropriately. The results support our hypothesis that such identification of symmetric features of the face can enhance the face recognition process. As the symmetry between the hemi faces is the core idea of this research, hence this method shows better results in LFW or age-based datasets (AgeDB, CA-LFW) but shows comparable results in the datasets focused on challenging side pose recognition (CP-LFW, CFP-FP). This further opens a new area of investigation to study pose-variant face samples in conjunction with symmetrical aspects.

7. Limitations

7.1. Training Time

This approach can work only in datasets comprising at least 20-30 % front-oriented face images. Another shortcoming is that this method employs additional training samples due to the face split process, which increases the training samples during the training phase. Though the inference time is always constant, we will explore further optimization of the SymFace loss in the future.

7.2. Societal Impacts

We stress that we do not condone or support the use of our work for mass surveillance and other repressive activities. We encourage the community and policymakers to establish clear regulations to prevent misuse. To mitigate this risk of False positives in security-related applications, we recommend deploying SymFace as part of a multi-factor authentication system, where facial recognition is one of several layers of security. In the context of our research, we

Loss Function	Inter-Class
ArcFace	1.23
ArcFace + SymFace	3.09

Table 3. Inter-class variance analysis on CASIA-WebFace on MobilefaceNet

Method	LFW Accuracy
AdaFace	99.8
Split with AdaFace	99.82
Split with AdaFace+SymFace	99.85

Table 4. Comparison study of symmetrical loss With ResNet100 and AdaFace on WebFace4M dataset

utilize the MS1MV* training dataset [7], which is sourced from MS-Celeb, a dataset that its creator has officially withdrawn due to ethical concerns. Using MS1MV* allows us to conduct a fair and rigorous comparison of our findings against state-of-the-art methodologies in the field. We only use the MS1MV dataset to compare the results in our research.

References

- [1] Yong Zhi Foo, Leigh W. Simmons, and Gillian Rhodes. Predictors of facial attractiveness and health in humans. *Scientific Reports*, 7(1):39731, Feb 2017. [1](#)
- [2] Wei Wei, Edmond S. L. Ho, Kevin D. McCay, Robertas Damaševičius, Rytis Maskeliūnas, and Anna Esposito. Assessing facial symmetry and attractiveness using augmented reality. *Pattern Analysis and Applications*, 25(3):635–651, Aug 2022. [1](#)
- [3] B er enice Delor, Fabien D’Hondt, and Pierre Philipot. The influence of facial asymmetry on genuineness judgment. *Frontiers in Psychology*, 12, 2021. [1](#)
- [4] Justyna Chojdak-Lukasiewicz and Bogusław Paradowski. Facial asymmetry: A narrative review of the most common neurological causes. *Symmetry*, 14(4), 2022. [1](#)
- [5] Gen Li, Yun Cao, and Xianfeng Zhao. Exploiting facial symmetry to expose deepfakes. In *2021 IEEE International Conference on Image Processing (ICIP)*, pages 3587–3591, Sep. 2021. [1](#)
- [6] Dong Yi, Zhen Lei, Shengcai Liao, and Stan Z. Li. Learning face representation from scratch. *CoRR*, abs/1411.7923, 2014. [1](#)
- [7] Yandong Guo, Lei Zhang, Yuxiao Hu, Xiaodong He, and Jianfeng Gao. Ms-celeb-1m: A dataset and benchmark for large-scale face recognition. In Bastian Leibe, Jiri Matas, Nicu Sebe, and Max Welling, editors, *Computer Vision – ECCV 2016*, pages 87–102, Cham, 2016. Springer International Publishing. [1](#), [8](#)
- [8] Soumyadip Sengupta, Jun-Cheng Chen, Carlos Castillo, Vishal M. Patel, Rama Chellappa, and David W. Jacobs. Frontal to profile face verification in the wild. In *2016 IEEE Winter Conference on Applications of Computer Vision (WACV)*, pages 1–9, 2016. [2](#), [5](#)
- [9] Tianyue Zheng and Weihong Deng. Cross-pose lfw : A database for studying cross-pose face recognition in unconstrained environments. In *Cross-Pose LFW : A Database for Studying Cross-Pose Face Recognition in Unconstrained Environments*, 2018. [2](#), [5](#)
- [10] Gary B. Huang, Manu Ramesh, Tamara Berg, and Erik Learned-Miller. Labeled faces in the wild: A database for studying face recognition in unconstrained environments. Technical Report 07-49, University of Massachusetts, Amherst, October 2007. [2](#), [5](#)
- [11] Stylianos Moschoglou, Athanasios Papaioannou, Christos Sagonas, Jiankang Deng, Irene Kotsia, and Stefanos Zafeiriou. Agedb: The first manually collected, in-the-wild age database. In *AgeDB: The First Manually Collected, In-the-Wild Age Database*, pages 1997–2005, 07 2017. [2](#), [5](#)
- [12] Tianyue Zheng, Weihong Deng, and Jiani Hu. Cross-age LFW: A database for studying cross-age face recognition in unconstrained environments. *CoRR*, abs/1708.08197, 2017. [2](#), [5](#)
- [13] Sinjini Mitra, Nicole A. Lazar, and Yanxi Liu. Understanding the role of facial asymmetry in human face identification. volume 17, pages 57–70, Mar 2007. [2](#)
- [14] Shui-Guang Tong, Yuan-Yuan Huang, and Zhe-Ming Tong. A robust face recognition method combining

Threshold value	Cross-posed images % (MS1MV2)	Cross-posed images % (WebFace4M)
0.05	38 %	42 %
0.1	48 %	54 %
0.2	59 %	66 %
0.3	66 %	73 %
0.4	74 %	78 %

Table 5. Proportions of cross-posed or non-front aligned faces in the different datasets

- lbp with multi-mirror symmetry for images with various face interferences. volume 16, pages 671–682, Oct 2019. 2
- [15] Muhammad Sajid, Imtiaz Ahmad Taj, Usama Ijaz Bajwa, and Naeem Iqbal Ratyal. Facial asymmetry-based age group estimation: Role in recognizing age-separated face images. *Journal of Forensic Sciences*, 63, 2018. 3
- [16] Yandong Wen, Kaipeng Zhang, Zhifeng Li, and Yu Qiao. A discriminative feature learning approach for deep face recognition. In Bastian Leibe, Jiri Matas, Nicu Sebe, and Max Welling, editors, *Computer Vision – ECCV 2016*, pages 499–515, Cham, 2016. Springer International Publishing. 3
- [17] Binghui Chen, Weihong Deng, and Junping Du. Noisy softmax: Improving the generalization ability of dcnn via postponing the early softmax saturation. In *2017 IEEE Conference on Computer Vision and Pattern Recognition (CVPR)*, pages 4021–4030, 2017. 3
- [18] Jiankang Deng, Yuxiang Zhou, and Stefanos Zafeiriou. Marginal loss for deep face recognition. In *2017 IEEE Conference on Computer Vision and Pattern Recognition Workshops (CVPRW)*, pages 2006–2014, 2017. 3
- [19] Feng Wang, Xiang Xiang, Jian Cheng, and Alan Loddon Yuille. Normface: L2 hypersphere embedding for face verification. *Proceedings of the 25th ACM international conference on Multimedia*, 2017. 3
- [20] Weiyang Liu, Yandong Wen, Zhiding Yu, and Meng Yang. Large-margin softmax loss for convolutional neural networks. In *International Conference on Machine Learning*, 2016. 3
- [21] Feng Wang, Jian Cheng, Weiyang Liu, and Haijun Liu. Additive margin softmax for face verification. *IEEE Signal Processing Letters*, 25(7):926–930, 2018. 3
- [22] Hao Wang, Yitong Wang, Zheng Zhou, Xing Ji, Dihong Gong, Jingchao Zhou, Zhifeng Li, and Wei Liu. Cosface: Large margin cosine loss for deep face recognition. In *2018 IEEE/CVF Conference on Computer Vision and Pattern Recognition*, pages 5265–5274, 2018. 3
- [23] Weiyang Liu, Yandong Wen, Zhiding Yu, Ming Li, Bhiksha Raj, and Le Song. Spheroface: Deep hypersphere embedding for face recognition. In *2017 IEEE Conference on Computer Vision and Pattern Recognition (CVPR)*, pages 6738–6746, 2017. 3
- [24] Jiankang Deng, Jia Guo, Niannan Xue, and Stefanos Zafeiriou. Arcface: Additive angular margin loss for deep face recognition. In *2019 IEEE/CVF Conference on Computer Vision and Pattern Recognition (CVPR)*, pages 4685–4694, 2019. 3, 5, 6
- [25] Yuge Huang, Yuhan Wang, Ying Tai, Xiaoming Liu, Pengcheng Shen, Shaoxin Li, Jilin Li, and Feiyue Huang. Curricularface: Adaptive curriculum learning loss for deep face recognition. In *2020 IEEE/CVF Conference on Computer Vision and Pattern Recognition (CVPR)*, pages 5900–5909, 2020. 3
- [26] Minchul Kim, Anil K. Jain, and Xiaoming Liu. Adaface: Quality adaptive margin for face recognition. In *2022 IEEE/CVF Conference on Computer Vision and Pattern Recognition (CVPR)*, pages 18729–18738, 2022. 3, 5, 6
- [27] Andrew G. Howard, Menglong Zhu, Bo Chen, Dmitry Kalenichenko, Weijun Wang, Tobias Weyand, Marco Andreetto, and Hartwig Adam. Mobilenets: Efficient convolutional neural networks for mobile vision applications. *ArXiv*, abs/1704.04861, 2017. 3
- [28] Mark Sandler, Andrew Howard, Menglong Zhu, Andrey Zhmoginov, and Liang-Chieh Chen. Mobilenetv2: Inverted residuals and linear bottlenecks. In *2018 IEEE/CVF Conference on Computer Vision and Pattern Recognition*, pages 4510–4520, 2018. 3

- [29] Andrew Howard, Mark Sandler, Bo Chen, Weijun Wang, Liang-Chieh Chen, Mingxing Tan, Grace Chu, Vijay Vasudevan, Yukun Zhu, Ruoming Pang, Hartwig Adam, and Quoc Le. Searching for mobilenetv3. In *2019 IEEE/CVF International Conference on Computer Vision (ICCV)*, pages 1314–1324, 2019. 3
- [30] Kai Han, Yunhe Wang, Qi Tian, Jianyuan Guo, Chunjing Xu, and Chang Xu. Ghostnet: More features from cheap operations. In *2020 IEEE/CVF Conference on Computer Vision and Pattern Recognition (CVPR)*, pages 1577–1586, 2020. 3
- [31] Ningning Ma, Xiangyu Zhang, Hai-Tao Zheng, and Jian Sun. Shufflenet v2: Practical guidelines for efficient cnn architecture design. In Vittorio Ferrari, Martial Hebert, Cristian Sminchisescu, and Yair Weiss, editors, *Computer Vision – ECCV 2018*, pages 122–138, Cham, 2018. Springer International Publishing. 3
- [32] Fadi Boutros, Patrick Siebke, Marcel Klemt, Naser Damer, Florian Kirchbuchner, and Arjan Kuijper. Pocketnet: Extreme lightweight face recognition network using neural architecture search and multistep knowledge distillation. *IEEE Access*, 10:46823–46833, 2022. 3
- [33] Yidong Ma. Effective methods for lightweight image-based and video-based face recognition. In *2019 IEEE/CVF International Conference on Computer Vision Workshop (ICCVW)*, pages 2683–2688, 2019. 3
- [34] Jianyu Xiao, Guoli Jiang, and Huanhua Liu. A lightweight face recognition model based on mobilefacenet for limited computation environment. *EAI Endorsed Transactions on Internet of Things*, 7(27):1–9, Feb. 2022. 3, 5, 6
- [35] Mohamad Alansari, Oussama Abdul Hay, Sajid Javed, Abdulhadi Shoufan, Yahya Zweiri, and Naoufel Werghi. Ghostfacenets: Lightweight face recognition model from cheap operations. *IEEE Access*, 11:35429–35446, 2023. 3
- [36] Yoanna Martınez-Dıaz, Luis S. Luevano, Heydi Mendez-Vazquez, Miguel Nicolas-Dıaz, Leonardo Chang, and Miguel Gonzalez-Mendoza. Shufflenet: A lightweight face architecture for efficient and highly-accurate face recognition. In *2019 IEEE/CVF International Conference on Computer Vision Workshop (ICCVW)*, pages 2721–2728, 2019. 3, 5, 6
- [37] Fadi Boutros, Naser Damer, Meiling Fang, Florian Kirchbuchner, and Arjan Kuijper. Mixfacenets: Extremely efficient face recognition networks. In *2021 IEEE International Joint Conference on Biometrics (IJCB)*, pages 1–8, 2021. 3
- [38] Anjith George, Christophe Ecabert, Hatef Otrosi Shahreza, Ketan Kotwal, and S ebastien Marcel. Edgeface : Efficient face recognition model for edge devices. *IEEE Transactions on Biometrics, Behavior, and Identity Science*, 2024. 3
- [39] Yang Zhang, Simao Herdade, Kapil Thadani, Eric Dodds, Jack Culpepper, and Yueh-Ning Ku. Unifying margin-based softmax losses in face recognition. In *2023 IEEE/CVF Winter Conference on Applications of Computer Vision (WACV)*, pages 3537–3546, 2023. 3
- [40] J. Zhou, X. Jia, Q. Li, L. Shen, and J. Duan. Uni-face: Unified cross-entropy loss for deep face recognition. In *2023 IEEE/CVF International Conference on Computer Vision (ICCV)*, pages 20673–20682, Los Alamitos, CA, USA, oct 2023. IEEE Computer Society. 3
- [41] qiufu li, Xi Jia, Jiancan Zhou, Linlin Shen, and Jinming Duan. Unitsface: Unified threshold integrated sample-to-sample loss for face recognition. In A. Oh, T. Naumann, A. Globerson, K. Saenko, M. Hardt, and S. Levine, editors, *Advances in Neural Information Processing Systems*, volume 36, pages 32732–32747. Curran Associates, Inc., 2023. 3
- [42] Yichun Shi, Xiang Yu, Kihyuk Sohn, Manmohan Chandraker, and Anil K. Jain. Towards universal representation learning for deep face recognition. In *2020 IEEE/CVF Conference on Computer Vision and Pattern Recognition (CVPR)*, pages 6816–6825, 2020. 3
- [43] Mengjia Yan, Mengao Zhao, Zining Xu, Qian Zhang, Guoli Wang, and Zhizhong Su. Vargfacenet: An efficient variable group convolutional neural network for lightweight face recognition. In *2019 IEEE/CVF International Conference on Computer Vision Workshop (ICCVW)*, pages 2647–2654, 2019. 3
- [44] Yonghyun Kim, Wonpyo Park, and Jongju Shin. Broadface: Looking at tens of thousands of people at once for face recognition. In *European Conference on Computer Vision*, pages 536–552. Springer, 2020. 3
- [45] Yichun Shi and Anil Jain. Probabilistic face embeddings. In *2019 IEEE/CVF International Conference on Computer Vision (ICCV)*, pages 6901–6910, 2019. 3
- [46] Shen Li, Jianqing Xu, Xiaqing Xu, Pengcheng Shen, Shaolin Li, and Bryan Hooi. Spherical confidence

- learning for face recognition. In *2021 IEEE/CVF Conference on Computer Vision and Pattern Recognition (CVPR)*, pages 15624–15632, 2021. 3
- [47] Jiankang Deng, Jia Guo, Evangelos Ververas, Irene Kotsia, and Stefanos Zafeiriou. Retinaface: Single-shot multi-level face localisation in the wild. In *2020 IEEE/CVF Conference on Computer Vision and Pattern Recognition (CVPR)*, pages 5202–5211, 2020. 4, 5
- [48] Z. Zhu, G. Huang, J. Deng, Y. Ye, J. Huang, X. Chen, J. Zhu, T. Yang, J. Lu, D. Du, and J. Zhou. Webface260m: A benchmark unveiling the power of million-scale deep face recognition. In *2021 IEEE/CVF Conference on Computer Vision and Pattern Recognition (CVPR)*, pages 10487–10497, Los Alamitos, CA, USA, jun 2021. IEEE Computer Society. 5, 6
- [49] Mohammad Saeed Ebrahimi Saadabadi, Sahar Rahimi Malakshan, Ali Zafari, Moktari Mostofa, and Nasser M. Nasrabadi. A quality aware sample-to-sample comparison for face recognition. In *2023 IEEE/CVF Winter Conference on Applications of Computer Vision (WACV)*, pages 6118–6127, 2023. 6
- [50] Kaiming He, Xiangyu Zhang, Shaoqing Ren, and Jian Sun. Deep residual learning for image recognition. In *2016 IEEE Conference on Computer Vision and Pattern Recognition (CVPR)*, pages 770–778, 2016. 6
- [51] Sheng Chen, Yang Liu, Xiang Gao, and Zhen Han. Mobilefacenet: Efficient cnns for accurate real-time face verification on mobile devices. In Jie Zhou, Yunhong Wang, Zhenan Sun, Zhenhong Jia, Jianjiang Feng, Shiguang Shan, Kurban Ubul, and Zhenhua Guo, editors, *Biometric Recognition*, pages 428–438, Cham, 2018. Springer International Publishing. 7